



Groundwater investigation through vertical electrical sounding: a case study from southwest Neyveli Basin, Tamil Nadu

S. Vijayaprabhu¹ · S. Aravindan² · K. Kalaivanan¹ · S. Venkatesan³ · R. Ravi²

Received: 22 September 2021 / Accepted: 17 January 2022 / Published online: 1 February 2022
© Islamic Azad University (IAU) 2022

Abstract

The Schlumberger technique with four electrode configurations was used to conduct an electrical resistivity study at different locations. A total of 27 vertical electrical sounding (VES) tests were carried out during the study, with each test representing a distinct litho unit being examined. The data collected were analyzed and interpreted using the curve matching method with the IPI2Win software. From the result, 22% of VES locations dominated by H ($\rho_1 > \rho_2 < \rho_3$) type (VES 2, 5, 6, 11, 21, 22), indicating potential water sites and QH type (VES 3, 7, 10, 20, 23, 24) indicating complex lithology overlain by softer strata, which can be an excellent local for the groundwater potential zone. 19% of HK type (VES 8, 9, 15, 16, 19) indicating $\rho_1 > \rho_2 < \rho_4 > \rho_4$. A-type curves ($\rho_1 < \rho_1 < \rho_3$; VES 1, 4, 17, and 18) fell in 15% of the area, signifying complex rock with poor terrain for groundwater storage. Based on this interpretation, this study shows the effectiveness of the electrical resistivity method in identifying prospective groundwater zones. It is determined by resistivity of saltwater enriched sediments, clay containing moderate freshwater, and freshwater carrying formations are present. Salty, moderate-fresh, and freshwater aquifers are easily identified with the D–Z characteristics. Thus, the spatial behavior of the D–Z parameters confirmed the presence of salty and freshwater aquifer structures in coastal aquifers. This method is highly recommended for areas with a comparable geological setting like the one developed.

Keywords Vertical electrical sounding (VES) · Iso-resistivity · Groundwater potential zone · Aquifer

Introduction

Groundwater perception has exceeded the safe yield in many parts of the world, resulting in overexploitation and over-emphasizing the aquifer (Chatterjee & Purohit, 2009; Hazarika & Nitivattananon, 2016; Maity et al., 2017). Therefore, the quantum of available groundwater resources has to be assessed accurately for its optimum extraction and utilization. Groundwater crisis has been caused by human activities and demand for water in domestic use, agriculture, and manufacturing (Sampat, 2000). While water resources are a crucial problem, research shows that groundwater supplies

have been affected recently (Kalaivanan et al., 2018; Nagaraju et al., 2011).

Groundwater is dynamic as it grows with irrigation, industrialization, urbanization, etc. As it is the most accessible freshwater supply, it has become essential to focus on prospective groundwater and monitor and preserve critical groundwater resources (Chopra & Ramachandran, 2021; Latha et al., 2010). Geoelectrical resistivity techniques are also used to reveal structural parameters and define polluted groundwater zones, significant factors (Selvakumar et al., 2015). Resistivity methods can be used for groundwater investigations where good electrical Resistivity contrast exists between the water-bearing formations and the underlying rocks (Verma et al., 1980). Accurate and reliable results have been obtained when these methods are proposed with a thorough understanding of geological, geomorphologic, and hydrogeological environments, water table conditions, and topography in a specific location (Kavidha & Elangovan, 2013; Kolandhavel & Ramamoorthy, 2019; Panda et al., 2017). Four essential techniques are available: gravity, magnetic, seismic, and geoelectrical

✉ K. Kalaivanan
kalai.geo87@gmail.com

¹ Department of Geology, Bharathidasan University, Tiruchchirappalli, Tamil Nadu 620 023, India

² Department of Earth Sciences, Annamalai University, Annamalai Nagar, Tamil Nadu 608002, India

³ Department of Geology, National College, Tiruchchirappalli, Tamil Nadu 620 001, India

prospecting. This electrical resistivity method solves groundwater problems through its highest resolving power and economic viability. Electrical resistivity methods are used to investigate the different lithological formations, bedrock dispositions, depth to the water table or zone of saturated formations, thickness of weathered zones, detection of fissures, fractures, fault zones, and the establishment of their depths, thickness, and lateral extent of aquifers. Groundwater flow direction, valley fills and depth to the basement in hard rocks, fresh and saltwater intrusion, prospective groundwater zones for locating ore deposits, and archaeological studies (Lawal et al., 2020).

Many scholars have examined the issue from various perspectives. Using Schlumberger electrode configuration, groundwater data is integrated to detect subsurface features and water locations (Kalaivanan et al., 2019; Kumar & Yadav, 2015; Mondal, 2021; Ndatuwong & Yadav, 2015; Patil et al., 2020; Sathiyamoorthy & Ganesan, 2018; Senthilkumar et al., 2017, 2019; Singh et al., 2021; Suneetha & Gupta, 2018). It has been shown that the VES technique and 2D resistivity may be a superior tool in comprehending hydrogeological issues. The research area groundwater zones are identified using the electrical resistivity technique. The geophysical design now provides more meaningful information on subsurface geology. Geoelectrical methods also connect the hydraulic characteristics of aquifers and the geophysical parameters (hydraulic conductivity and transmissivity), including longitudinal conductance and transverse resistance (Bello et al., 2019; Mondal, 2021; Naidu et al., 2021).

Sustainable groundwater quantity and quality assessment have become more dependent on geophysical techniques, mainly electrical resistivity (Arunbose et al., 2021). The accessibility of the VES method has made it extremely popular in groundwater prospect and engineering investigations (Utom et al., 2012). The Electrical resistivity method helps determine different subsurface strata depth, thickness, and water yielding capacities (Gaikwad et al., 2021). The lithological characteristic and geology of the southwest Neyveli Basin must be known under hydrogeological conditions (Devaraj et al., 2018). Geophysical techniques also define and assess groundwater perspectives to understand sub-surface geology (Anbazhagan et al., 2015).

To determine fresh and saline water zones using the parameters S and T (Dar–Zarrouk parameters) (Bello et al., 2019; Mondal, 2021; Naidu et al., 2021; Senthilkumar et al., 2017). This study characterizes the aquifers and determines their depth in the southwest Neyveli Basin. Aquifer lateral extent and overburden protection capacity from surface contamination were determined employing D–Z parameters in the southwest Neyveli Basin, Cuddalore District, Tamil Nadu.

Study area

The southwest of Neyveli Basin is located in Cuddalore District, Tamil Nadu, India, and lies within the topographic sheets 58M/6, 58M/7, 58M/10, and 58M/11 published by the Survey of India (SOI) during the year 2011 on the scale of 1:50,000 between the latitude $11^{\circ} 25''$ – $11^{\circ} 45''$ and longitude $79^{\circ} 15''$ – $79^{\circ} 35''$ (Fig. 1). The areal extent of the West Neyveli Basin is 556.48 km². It is bounded in the north by Konjikuppam–Palakollai ridge and Gadilam river drainage basin, south by Vellar and Manimukthanadi, and East by Kumbakonam–Chennai National high ways and in the West by Virudhachalam Cretaceous in the southwest Neyveli Basin. The alluvial plain occupies the southeastern part of the study area, and northwestern (NW) part is made up of elevated, undulating terrains of Cretaceous Limestone and Cuddalore Sandstone rocks. The elevation ranges between 20 m in the south-southeast (SSE) to 100 m above mean sea level (MSL) in the Northwestern part. The highest elevation is found in Vedhakoil, with 106 m AMSL. The central high land area stretches roughly north-northeast to south-southwest in the basin's center. In the study area, high land stretches from NNE–SSW in the western part of the basin.

Geological setting of the study area

The occurrence and movement of groundwater depend upon several factors like the topography of the terrain, geological setup, structural disturbances, soil types, structural pattern, rainfall, etc. with the help of the topographic map, surface geology is studied in detail, and the boundaries of various lithological units in southwest Neyveli Basin are demarcated. Different geological formations underline the study area with age from Mesozoic to recent sediments. Sedimentary rock types of the Ariyalur group mainly cover the basin as two formations they are:

Cuddalore formation

Tertiary period of Mio-Pliocene age, which occupies about 414.38 km² of Miocene sandy clay and 1.52 km² of laterites in total within Cuddalore sandstone (415.90 km²) shown in Fig. 1. It consists of lateritic sandstone, clay, sand, silt, etc.

Aladi formation

A Mesozoic period of cretaceous age assemblage it consists of clay (29.57 km²), calcareous sandstone of (0.98 km²), and sandy limestone of (1.94 km²).

The remaining part of the study area comprises Quaternary fluvial deposits with age from Pleistocene to Holocene

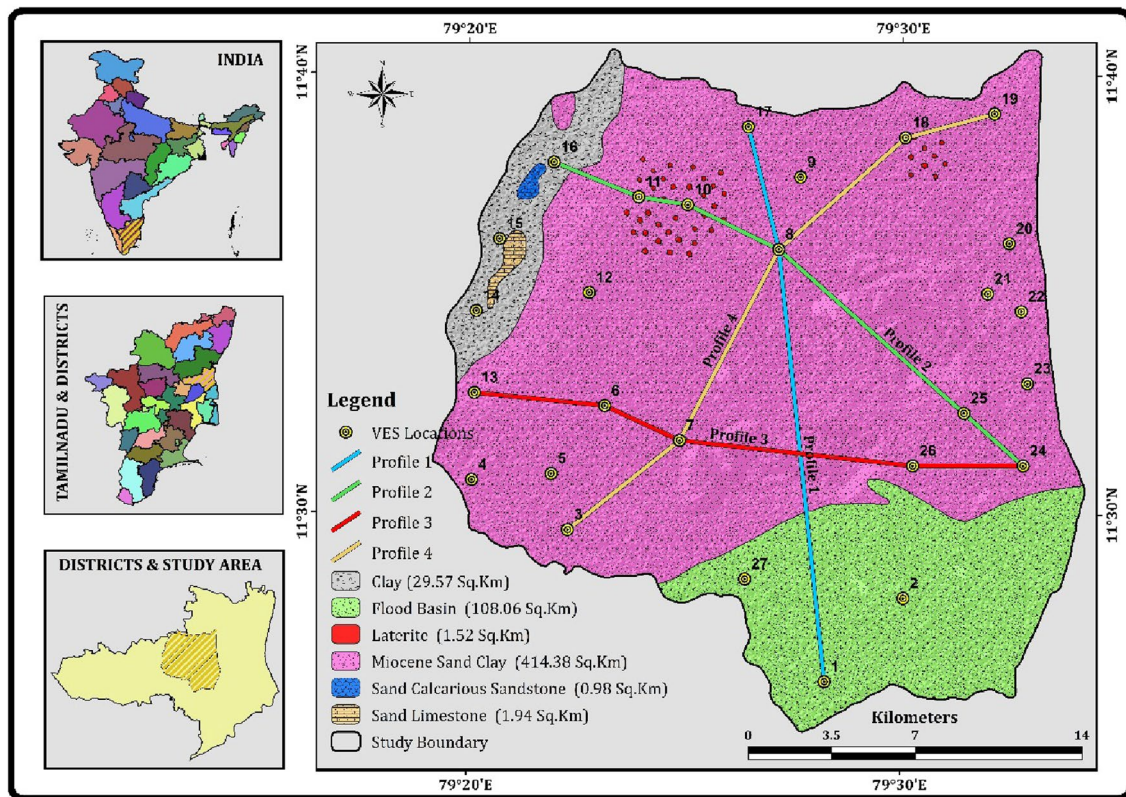


Fig. 1 Geology and VES location map of the study area

is covered by river alluvium and recent sediment deposits (108.06 km^2). The geology of the study area was checked during field investigations with the help of a geological map of the Cuddalore District, published by the Geological Society of India.

Materials and methods

The southwest, Neyveli Basin boundary, was digitized using the topographic maps and registered with the help of the GIS environment. Survey of India (SOI) topographic maps, viz., 58M/6, 58M/7, 58M/10, and 58M/11 on a 1:50,000 scale were used. For evaluating the potential groundwater zones in the investigated area, it was discovered that there were 27 VES that could be assessed using the Schlumberger electrode array, which was used in this study (Fig. 1). Schlumberger Configuration Survey concepts were addressed by many authors (Gopinath & Srinivasamoorthy, 2014; Gopinath et al., 2017, 2018; Mathiazhagan et al., 2015; Nageswara Rao et al., 2018; Prabhu & Sivakumar, 2018; Ravi et al., 2021). All VES were measured using the SSR-MP-AT-ME (CM) equipment, with a maximum current electrode spacing of 100 m. Data

from the gathered samples were analyzed using the IPI-2win software to determine the model layers. The apparent resistivity data generated iso-apparent resistivity and iso-layer thickness spatial maps at different AB/2 spacing. Besides, to better understand subsurface lithological variation and delineate freshwater aquifer zones, an attempt has been made to prepare pseudo-sections and develop a relative resistivity model of the study area.

The Dar–Zarrouk (D–Z) characteristics, including cross-unit resistance (T), longitudinal driving (S), longitudinal (SL), transverse resistivity (S_v), electrical anisotropy, and root average square resistivity (S_m), were investigated in this study using VES data (Ayolabi et al., 2010; Singh et al., 2021). The longitudinal unit conductance (S) is parallel to the face for a cross-sectional unit area, which is critical for resistivity sonority. The transverse unit (T) resistance is normal to the face. These values are sufficient to compute the potential surface distribution and, therefore, an electric resistivity graph (Golekar et al., 2021).

If there are n geoelectric layers of thickness h_1, h_2, \dots, h_n and resistivity $\rho_1, \rho_2, \rho_3, \dots, \rho_n$ for a unit block of $H = \sum_{i=1}^n h_i$ square area and thickness (Patil et al., 2018). The S and T are equivalent to an anisotropic block with a square unit such that the unit resistance

$$S = \rho_1 h_1 + \rho_2 h_2 + \rho_3 h_3 + \dots + \rho_n h_n = \sum_{i=1}^n \rho_i h_i. \quad (1)$$

Transverse unit conductance

$$S = (h_1/\rho_1) + (h_2/\rho_2) + (h_3/\rho_3) + \dots + (h_n/\rho_n) = \sum_{i=1}^n (h_i/\rho_i). \quad (2)$$

This equation describes the layers' transverse resistivity (ρ_t) when a current flows through them at right angles to the layers.

$$\rho_t = (T/H). \quad (3)$$

According to the following equation, the longitudinal resistivity (ρ_l) to the current flowing parallel to the layers is defined as

$$\rho_l = (H/S). \quad (4)$$

Electrical anisotropy (λ) is given by

$$\lambda = \sqrt{\rho_l/\rho_t}. \quad (5)$$

The variables listed were utilized to restrict the freshwater zones in the southwest Neyveli Basin and calculate the aquifer's protective capacity. The combination of layer resistivity and thickness in D–Z parameters S and T , as stated by Patil et al., (2018), may be directly utilized to conduct aquifer protection studies and evaluate the aquifer's hydro-logic characteristics.

A geographic information system (GIS) was used to create a geodatabase containing the acquired data, then used to produce prediction maps using spatial analytic tools. These maps show the variance in apparent resistivity levels. The collected data were statistically evaluated, and calculation maps were produced using the statistical analyst of ArcGIS 10.8 software using the best IDW technique. The interpreted resistivity has been shown as a spatial map for the first layer, iso-apparent resistivity and its thickness.

Results and discussion

Interpretation of the vertical electrical sounding (VES)

The sub-basin VES data were interpreted using IPI-2Win software version 3.0.1 (Moscow State University 1990–2003), and the interpreted sounding curves are shown in Fig. 2. Table 1 shows the layer-wise aquifer thickness and resistivity. However, five-layer curves were also derived from the interpretation. The resistivity value of the first layer varies from 1.71 to 1135 Ωm and the second layer resistivity

varies from 0.236 to 1165 Ωm . The subsurface layer thickness of the first and second layers varies from 0.75 to 7.06 and 0.503 to 253 m, respectively. Similarly, the resistivity value range for the third and fourth layers are 0.0018–53,866 and 0.0012–5509 Ωm respectively. Likewise, the subsurface thickness of the third and fourth layers varies from 0.904 to 51.3 and 8.06 to 49.9 m. The fifth layer resistivity varies from 0.0083 to 5379 Ωm (Table 1). The RMS error percentage was less than 10 in all VES locations.

The vertical electrical sounding (VES) data were interpreted quantitatively and qualitatively. To determine the depth of the layers by using their respective thickness and resistivity (Gopinath et al., 2017; Kalaivanan et al., 2019). Using VES data, the curve matching technique has been analyzed using IPI2Win software for 27 locations. In the study area, obtained sounding curves are shown in Table 2. According to the findings, 22% of VES locations are dominated by the H ($\rho_1 > \rho_2 < \rho_3$) type (VES 2, 5, 6, 11, 21, 22), indicating potential water sites. The QH type (VES 3, 7, 10, 20, 23, 24), indicating hard lithology overlain by softer strata, which can be a good local for the groundwater potential zone (hard lithology overlain by softer strata). 19% of HK type (VES 8, 9, 15, 16, 19) indicating $\rho_1 > \rho_2 < \rho_3 > \rho_4$. A-type curves ($\rho_1 < \rho_2 < \rho_3$; VES 1, 4, 17 and 18) were fall in 15% of the area which signifying hard rock terrain (Patil et al., 2020), 7% K (VES 14, 26), KQ type ($\rho_1 < \rho_2 > \rho_3 > \rho_4$; VES 12, 27) and 4% HA type ($\rho_1 > \rho_2 < \rho_3 < \rho_4$; VES 13) QQ type (VES 25), Fig. 3 and Table 2. When a resistant surface has been present, this kind of curve shows relatively resistant topsoil as well as a saturated aquifer zone. According to Omosuyi et al. (2021), the H and KH type VES curves reflect the unconfined weathered, confined weathered, and fractured aquifers, respectively, in a given region. As a result, all curve types include H or K types, suggesting that groundwater accumulation and storage are adequate.

Iso-resistivity and thickness

The apparent resistivity values and the thickness have been distributed spatially to develop a resistivity map to get an overall spatial perspective of the study area. The resistivity and thickness values for the first layer varied from less than 1.71–1135 Ωm and 0.75–7.06 m, respectively. In the first layer, the low resistivity value is noted in VES-4 (Bhudhamur), probably due to the presence of clay. The higher value observed in VES-8 (Dhidirkuppam) may be due to the occurrence of laterites. Minimum layer thickness has been identified as 0.75 m due to the occurrence of topsoil in VES-25 (Seplanatham). The maximum layer thickness of 7.06 m is noted in VES-14 (Chitherikuppam) due to limestone. The spatial variation of resistivity has also been attempted to recognize the topsoil thickness and lithological control. The first layer shows that less than 20 Ωm resistivities are

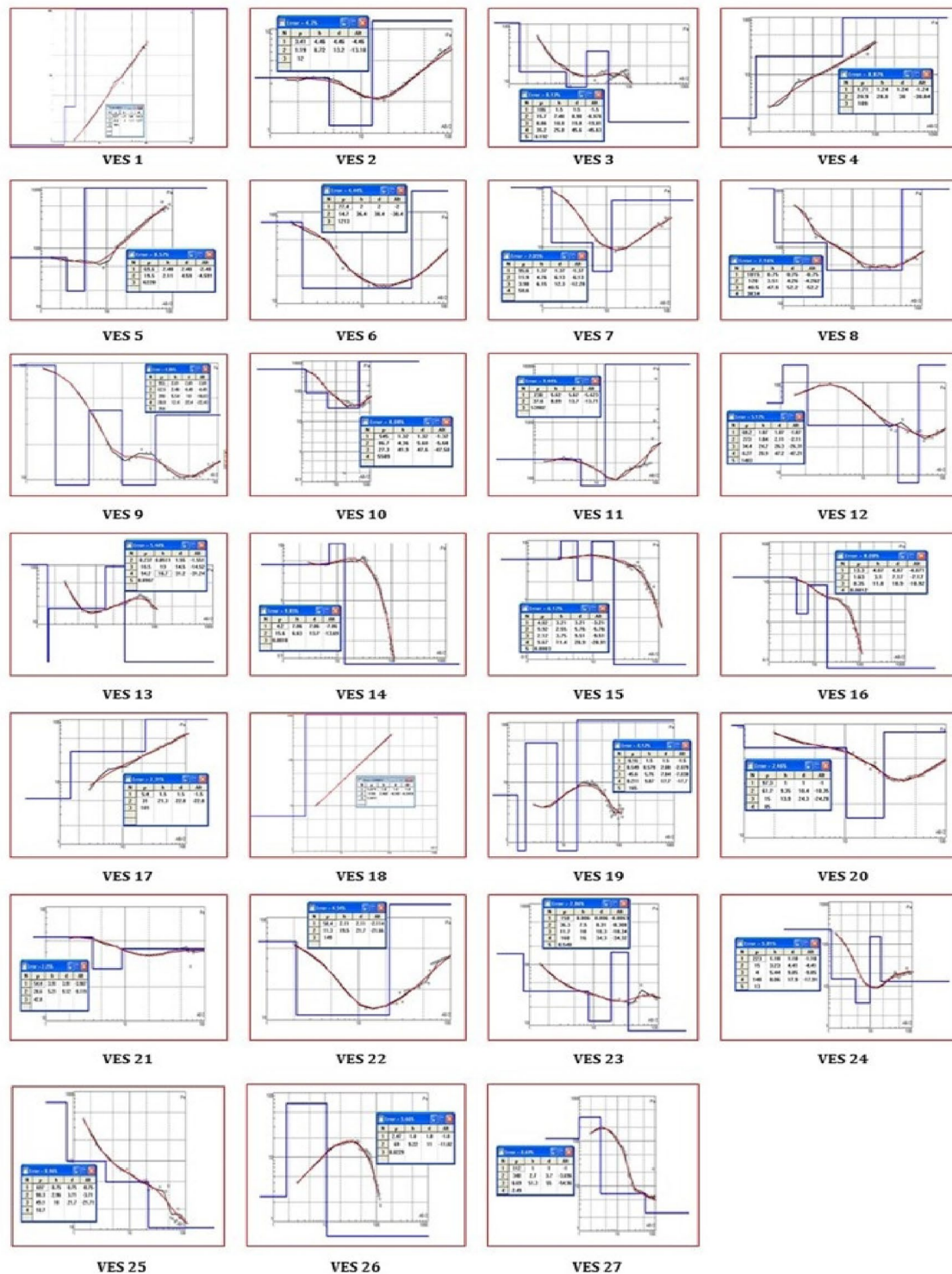


Fig. 2 VES curves of the study area

observed as isolated spots in the eastern and western part of the study area (Fig. 4). The 20–60 Ωm resistivity range is also observed as isolated patches in the eastern and western parts of the study area. The higher resistivity of greater than

120 Ωm followed by more than 1000 Ωm was noticed as enclosed patches in the central part of the study area near Vedhakovil. The spatial map of the first layer thickness has shown (Fig. 4) that less than 3 m is observed in most parts of

Table 1 Electrical resistivity and layer thickness of the study area

VES no.	VES locations	h_1	ρ_1	h_2	ρ_2	h_3	ρ_3	h_4	ρ_4	ρ_5	Error %	Curve type
1	AgaraAlambadi	1.82	6.87	1.3	33.4	∞	2910	∞	∞	∞	4.99	A
2	Dharmanallur	4.46	3.41	8.72	1.19	∞	14.3	∞	∞	∞	3.46	H
3	Ko—Adanur	1.5	106	7.44	15.7	10.7	8.85	25.8	35.2	0.192	8.15	QH
4	Boothampur	1.24	1.71	28.8	20.9	∞	109	∞	∞	∞	8.87	A
5	Pudukuraipettai	2.48	69.7	2.11	19.5	∞	6165	∞	∞	∞	8.58	H
6	Eruppukurichchi	2	77.4	36.4	14.7	∞	1213	∞	∞	∞	4.45	H
7	Kombadikuppam	1.37	95.6	4.76	11.9	6.15	3.98	∞	58.6	∞	2.07	QH
8	Dhidirkuppam	0.752	1135	0.665	55.6	0.904	334	49.9	41.2	5379	7.12	HK
9	Nandukuzhi	2.01	955	2.48	62.5	5.54	390	12.4	28.9	358	4.86	HK
10	Kovilankuppam	1.32	545	4.36	86.7	41.9	27.3	∞	5509	∞	8.08	QH
11	Vedakovil	5.62	230	8.11	37.6	∞	53,866	∞	∞	∞	9.44	H
12	Kotteri	1.07	60.2	1.04	273	24.2	34.4	20.9	8.27	1483	5.16	KQ
13	Kandiyankuppam	1.5	101	0.0503	0.236	12.9	18.4	16.7	94.4	0.0908	5.47	HA
14	Chitherikuppam	7.06	4.2	6.63	15.6	∞	0.0018	∞	∞	∞	9.85	K
15	Mattur	3.21	4.82	2.55	9.92	3.75	2.12	11.4	9.67	0.0083	6.09	HK
16	Aaladi	4.06	13.3	3.15	1.66	11.7	8.36	∞	0.0012	∞	8.06	HK
17	Kattugudalur	1.5	5.71	21.7	30.4	∞	104	∞	∞	∞	9.32	A
18	Sorattur	1.8	5.88	2.44	1165	∞	13,472	∞	∞	∞	0.69	A
19	Marungur	1.5	6.11	0.522	0.501	5.71	47.8	9.41	0.194	183	9.73	HK
20	Vadakkumelur	1	97.3	9.35	61.7	13.9	15	∞	85	∞	2.46	QH
21	Vanadirayapuram	3.91	54.4	5.21	28.6	∞	42.8	∞	∞	∞	2.25	H
22	Thenkuttu	2.11	58.4	19.6	11.3	∞	149	∞	∞	∞	4.54	H
23	VadalurSabai	0.812	149	253	36.2	10	11.7	16	160	0.555	7.86	QH
24	Karunkuzhi	1.18	223	3.23	15	5.44	4	8.06	148	13	5.8	QH
25	Seplanattam	0.75	697	2.96	98.3	18	49.1	∞	10.7	∞	8.96	QQ
26	Guruvesipuram	1.8	2.47	9.22	69	∞	0.0229	∞	∞	∞	5.67	K
27	Kammapuram	1	112	2.7	339	51.3	6.69	∞	2.49	∞	8.69	KQ

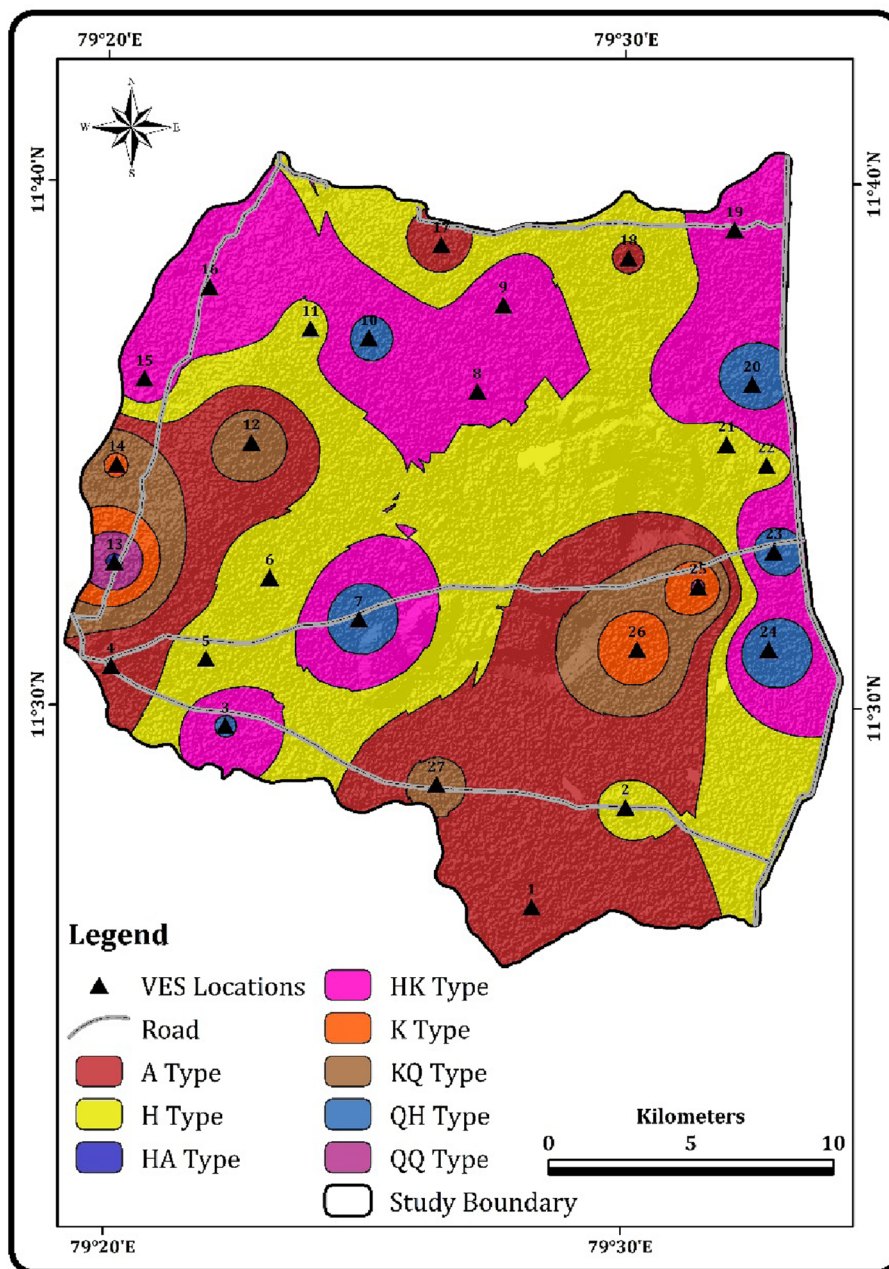
Table 2 Curve types

Sl. no.	Curve types	VES locations	Per-centage (%)
1.	A	1, 4, 17, 18	15
2.	H	2, 5, 6, 11, 21, 22	22
3.	QH	3, 7, 10, 20, 23, 24	22
4.	HK	8, 9, 15, 16, 19	19
5.	KQ	12, 27	7
6.	HA	13	4
7.	K	14, 26	7
8.	QQ	25	4

the study area. Similarly, 3–5 m layer thickness is noticed in the western region and a smaller portion in the southern part due to lime-rich sandstone and calcic rocks and the possible occurrence of aragonite minerals in the Northeastern part. In contrast, more than 5 m thickness is noticed as pockets in the western zone due to limestone.

The second layer's apparent resistivity and thickness vary from less than 1–1165 Ω m and 0.503–253 m thickness, respectively (Table 1). A shallow resistivity value of less than 0.234 Ω m in the second layer is observed in the VES location 13 (Kandiyankuppam) may be due to the probable occurrence of clay. The maximum resistivity value of 1165 Ω m is noted in VES location 18 (Sorathur) due to the possible occurrence of laterite as the second layer. The minimum layer thickness is observed in VES-13 (Kandiyankuppam), whereas the maximum thickness in VES-23 (Vadalur Sabai) is due to the occurrence of sand (Fig. 5). A spatial map of resistivity variation for the second layer occurs as small portions are observed in the study area. It exhibits a low resistivity of less than 20 Ω m. The resistivity range 20–60 Ω m is observed in the eastern and western part and as small patches in the center and eastern part of the study area. In the Central Zone, 60–120 Ω m resistivity values occur. It is due to the presence of coarse-grained arenaceous materials. High resistivity ranges are observed in the study area's Northern, Southern, and Western parts.

Fig. 3 Cure type spatial distribution



Similarly, the second layer thickness shows an approximately similar trend to the first layer. Still, the layer thickness is higher in the eastern and western parts of the study area. The maximum layer thickness of greater than 20 m is observed in the west-central zone, and thickness of 5–10 m is noticed in almost the central part of the study area (Fig. 5).

In the third layer, the resistivity ranges from less than 1–53,866 Ωm , and layer thickness varies from 0.904 to 51.3 m, respectively. The high resistivity was observed in VES-11(Vedakovil) due to laterite and low resistivity. In VES-14 (Chitherikuppam), for the likely clay with limestone. The layer thickness was found to be maximum in

VES-27 (Kammapuram) due to its proximity to the northern bank of the Vellar river, and minimum thickness was noticed in VES-8 (Dhidirkuppam) due to the probable occurrence of laterites. The spatial map of the third layer exhibits a maximum area under resistivity of less than 5000 Ωm is noticed in the north-central part and small enclosures in the southern part of the study area (Fig. 6). Resistivity value of 20–60 Ωm has shown as enclosures without closing off the contour due to the occurrence of fault from NW to SE from south of I and II mines of NLC towards SE. In the eastern part, between 20 and 60 and 60 and 120 Ωm , the contour is observed in the study area. Above 200 Ωm contours are

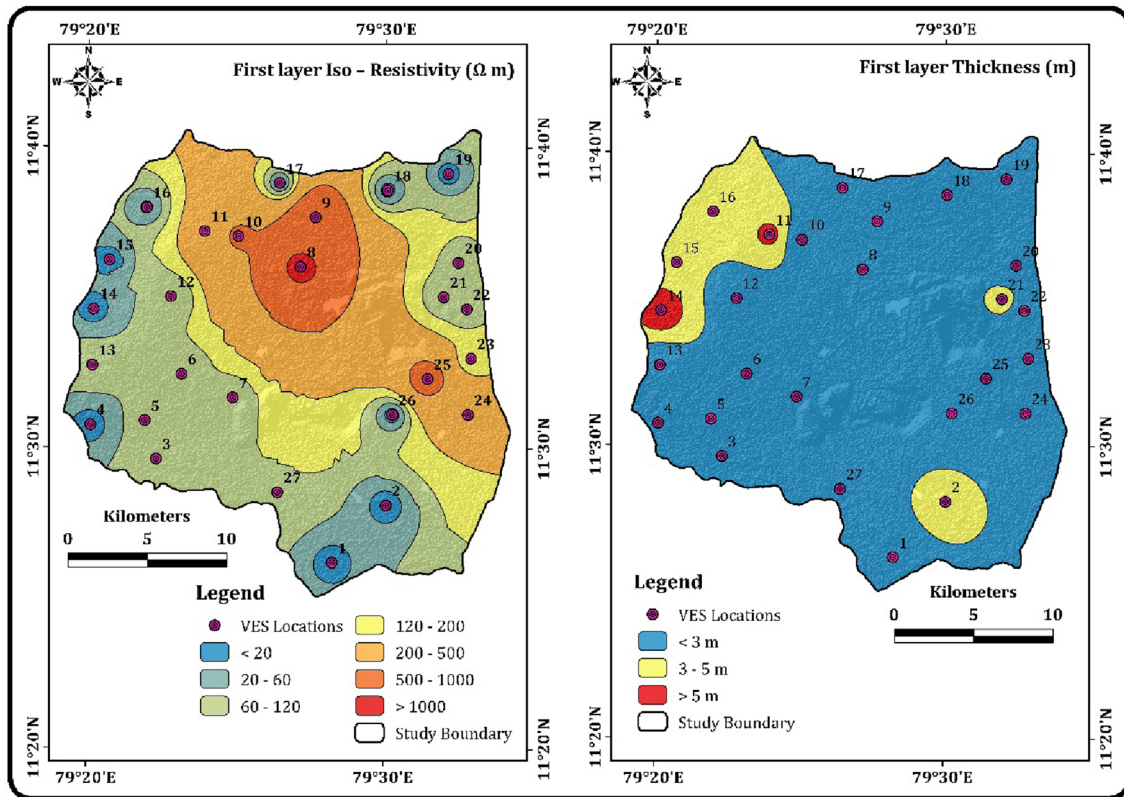


Fig. 4 Spatial distribution of first layer iso-resistivity and thickness

observed in the SE part of the study area. The layer thickness of less than 5 m is noticed along the study area's NE, SE, NW, and SW parts. Similarly, throughout the study area, the layer thickness of 5–10 m occur. In contrast, more than 50 m thickness is observed as a small patch adjacent to Manimukthanadhi in the northern bank of the study area (Fig. 6).

The fourth layer resistivity varies from less than 1–5509 Ωm . The high resistivity was observed in VES-10 (Kovilankuppam), whereas the low resistivity was observed in VES-16 (Aladi). The layer thickness was encountered with a maximum thickness of 49.9 m in VES-8 (Thidirkuppam) and a minimum layer thickness of 8.06 m found in VES-26 (Karukuzhi, Table 1). The resistivity variation in the fifth layer was observed as 5379 Ωm in VES-8 (Thidirkuppam) and less than 1 Ωm in VES-15 (Mattur).

The resistivity value was very high in a few locations, irrespective of layers. In general, resistivity anomaly is rare, particularly in the sedimentary terrain. Keller and Frischknecht (1966), the resistivity in Terrestrial Sedimentary formations may vary from 1 to 300 Ωm . For marine sediments, it is less than 300 Ωm . But, in the study area, the first layer resistivity value of above 1000 Ωm has been observed only in VES-8 (Dhidirkuppam). It is due to the occurrence of laterites. Similarly, in the second layer, high resistivity of 1165 Ωm has been noticed in VES-18 (Sorathur). In the

third layer, 53,866 Ωm has been inferred in VES-11 (Vedakovil) due to acidic laterites, respectively.

In the fourth and fifth layers, high resistivity of 5509 Ωm has been observed in VES-10 (Kovilankuppam). In the fifth layer, high resistivity of 5379 Ωm is observed in VES-08 (Dhidirkuppam) due to the influence of laterites. The higher resistivity value obtained at the top layer and shallow depths in certain areas are mainly due to dry loosened sand on the top layer. It is due to acidic laterite derivatives and dry compact sandy clay formations. The low resistivity value obtained indicates the presence of wet clay and clayey sand formations. Abnormal high resistivity in specific locations could be due to acidic laterites and gravel deposits saturated. Low ionic strength groundwater is the primary factor for high resistivity in the study area.

Pseudo-sections and resistivity model

An attempt was made to prepare pseudo-sections to understand the subsurface lithological variation better and locate potential aquifers of the study area. The create resistivity models of various profiles are shown in Fig. 1. According to the availability of electrical resistivity locations in multiple directions to produce a reliable output, the area was divided into four sections to represent in four directions,

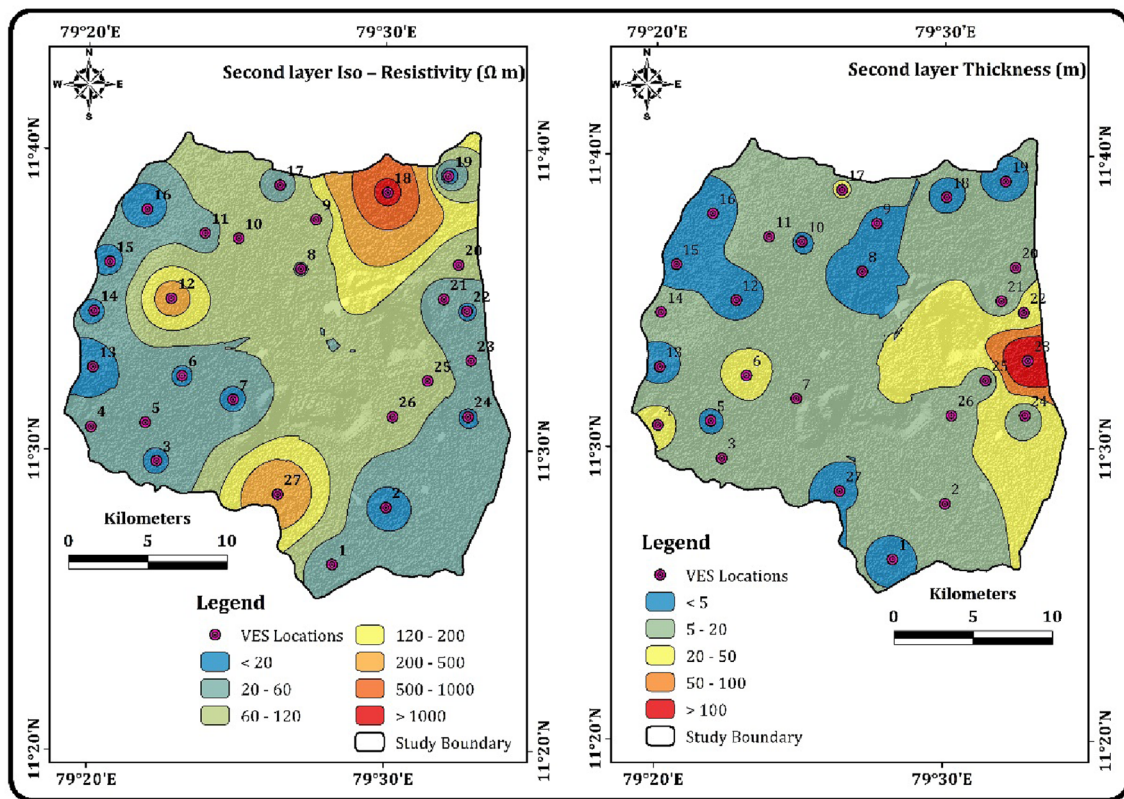


Fig. 5 Spatial distribution of second layer iso-resistivity and thickness

namely north–south section (profile 1), northwest to southeast (profile 2), east–west (profile 3), and northeast to southwest (profile 4) with data input to generate pseudo-sections.

Profile 1 (NS)

The profile-1 trending towards N–S directions, with VES locations 1, 8, and 17 (Fig. 7). VES 1 indicates, low resistivity of less than $27 \Omega\text{m}$ was noticed in the southern part to infer the possible occurrence of sand. The resistivity progressively increases with an increasing depth ranging from 35 to $275 \Omega\text{m}$, indicating calcium-rich sand to dry sand around Agara Alambadi in the southern part. The VES 17 and 8 show that maximum resistivity value was observed in the Northern part at a depth of 1–5 m to interpret the possible occurrence of lateritic exposure in and around Kattugudalur.

Profile 2 (NW–SW)

The pseudo section of profile-2 is shown in Fig. 8. In the second profile trending towards NW–SW directions (VES 8, 10, 11, 16, 24, and 25). The overall resistivity varies from less than 4– $250 \Omega\text{m}$, and the depth of investigation is 100 m from ground level. A low resistivity value of less

than $10 \Omega\text{m}$ was found up to 100 m from the surface in the western part in Aladi (VES 16). In contrast, in the middle position, it was observed as a thin pinch approximately at 17 m depth adjacent to Kovilankuppam (VES10). The resistivity gradually increased from $100 \Omega\text{m}$ from the shallow depth of 10–100 m below ground level (bgl) depth up to high resistivity of $250 \Omega\text{m}$ adjacent to Kovilankuppam. In the middle part, the resistivity ranges from 25 to $100 \Omega\text{m}$ was observed from 10 to 100 m bgl in the central region in and around Dhidirukuppam (VES 8). The resistivity range was observed from 25 to $40 \Omega\text{m}$ in Seplanatham (VES 25).

Profile 3 (EW)

The pseudo-resistivity section profile-3 trending towards EW direction (VES 6, 7, 13, 24, and 26) shown in Fig. 9. In lower resistivity value was observed in the central part with less than $14 \Omega\text{m}$ in and around Kombadikuppam (VES 7) with the probable occurrence of clayey sand, followed by $30\text{--}50 \Omega\text{m}$ with the possible event of coarse-grained sand was noticed at the western part of the study area in and around Eruppukurichi (VES 6). The higher range of resistivity value from 50 to $200 \Omega\text{m}$ with the possibility of dry sand to laterite was found in the eastern part within the top 4 m in and around Karunkuzhi (VES 24).

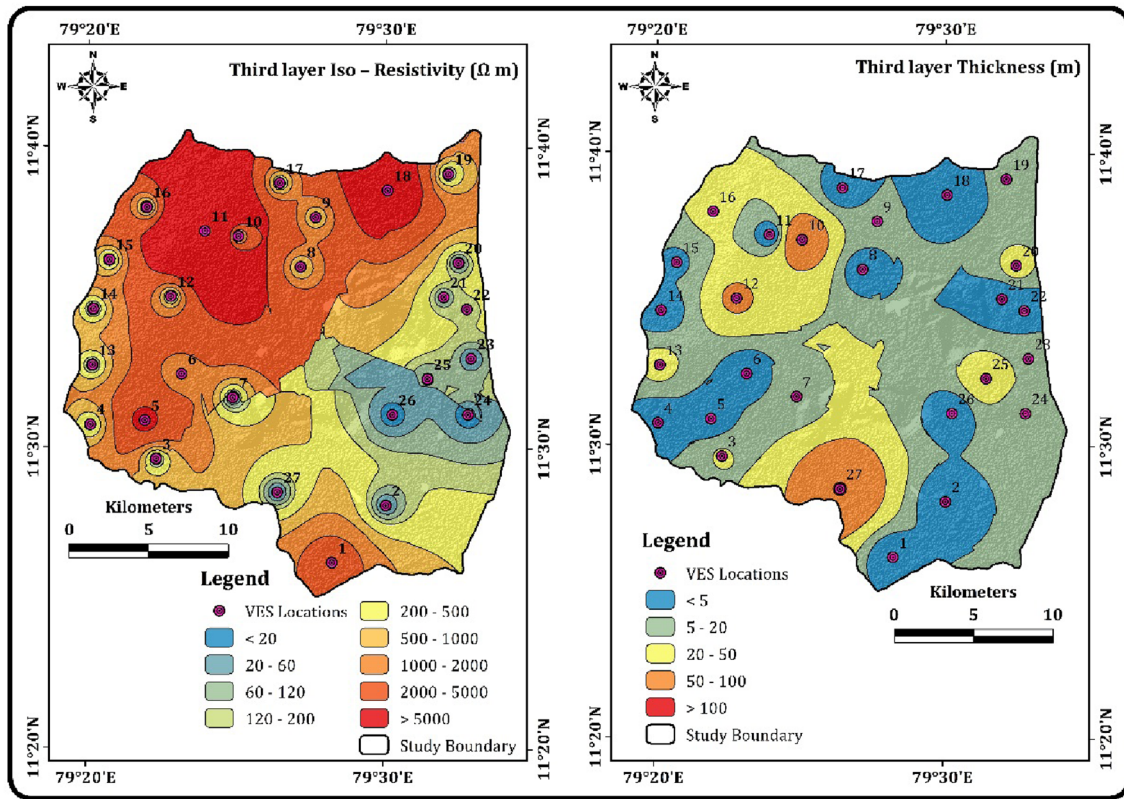


Fig. 6 Spatial distribution of third layer iso-resistivity and thickness

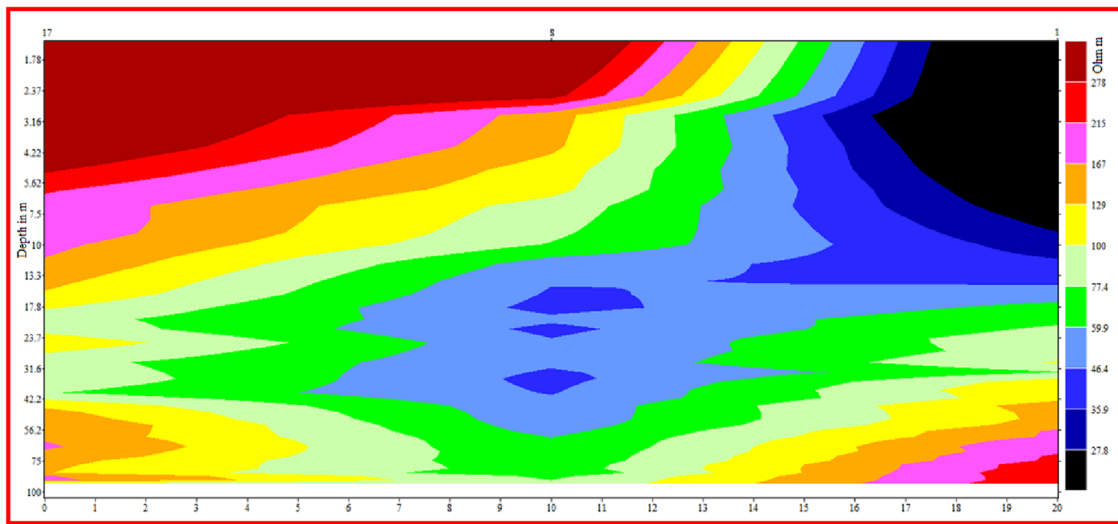


Fig. 7 NS pseudo sections of south west Neyveli Basin

Profile 4 (NE–SW)

The profile-4 trending towards NE–SW (VES 3, 7, 8, 18, and 19) direction shown Fig. 10. The resistivity range of less than 20 Ωm was observed in the third pseudo section,

and low resistivity of less than 20 Ωm was noticed in the Northeastern part in the proximity of Kombadikuppam (VES 7), and it extends towards the southwestern part. In the northwestern region, high resistivity of > 140 Ωm was

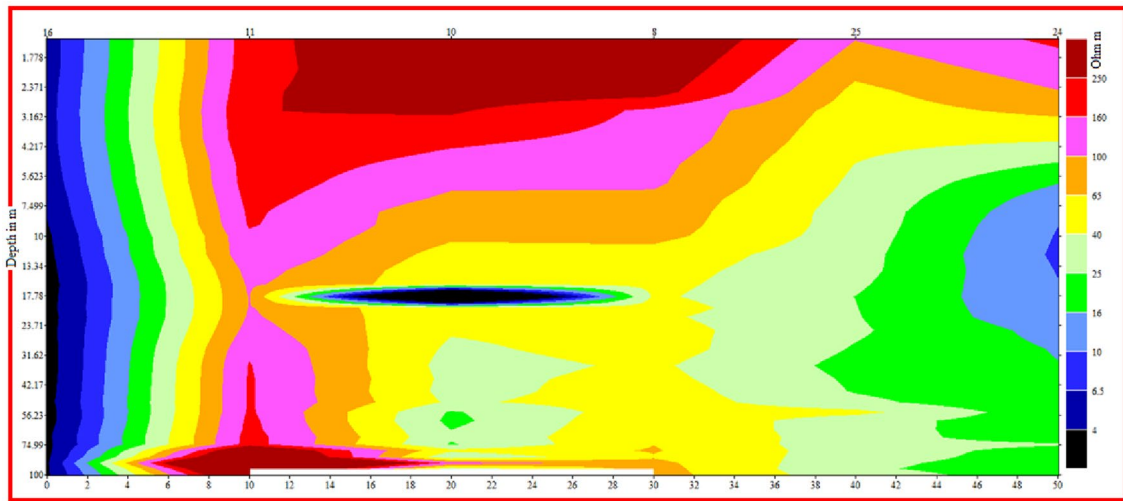


Fig. 8 NW–SE pseudo sections of south west Neyveli Basin

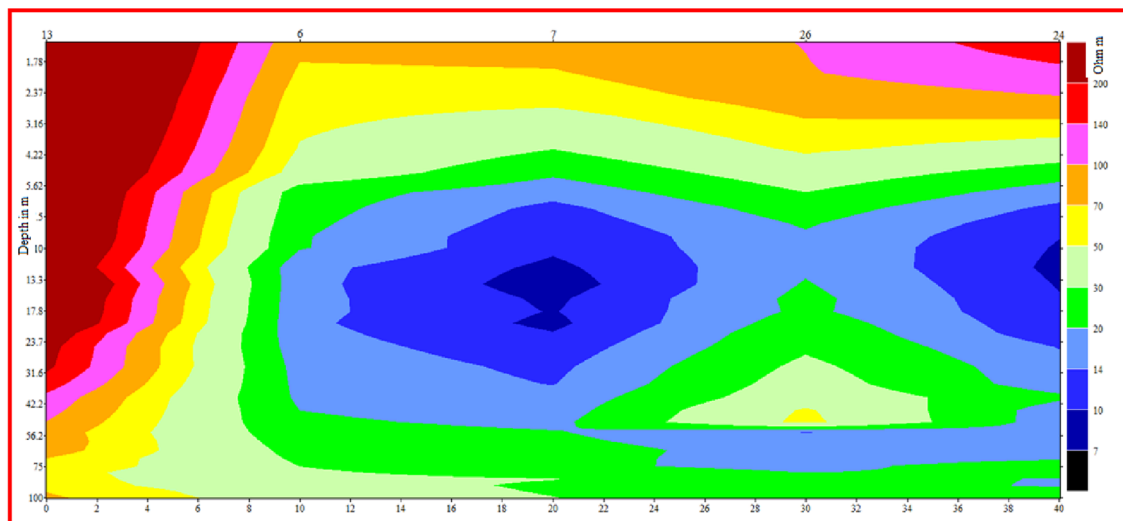


Fig. 9 EW pseudo sections of south west Neyveli Basin

observed as the top layer, and it increases gradually up to $300 \Omega\text{m}$ in the extreme northwest.

The relative resistivity model clearly distinguishes and demarcates high groundwater potential areas from moderate or low groundwater potential areas, which is indicated by various shades of colours related to different resistivity ranges. Red zone as higher groundwater potential zones with $141 \Omega\text{m}$ and above in and around Kandiyankuppam in the west. The yellow region indicates moderate groundwater potential zones ($50\text{--}70 \Omega\text{m}$). Green occurs below moderate potential zones with a resistivity of $11\text{--}30 \Omega\text{m}$ with sandy clay in Guruvesipuram in the east. The blackish-blue poor groundwater potential zone of $1\text{--}10 \Omega\text{m}$ indicates the clayey

formation in and around Karunkuzhi in the extreme east (Fig. 10).

Assessment of Dar–Zarrouk (D–Z) parameters

A geoelectric layer is described by two fundamental parameters, its resistivity (ρ) and thickness (h) of the sub-surface layer. Some other important D–Z parameters which can be derived from the layers resistivities and their thickness are total longitudinal unit conductance (S), total transverse unit resistance (T), aquifer anisotropy (λ) to identify the potential

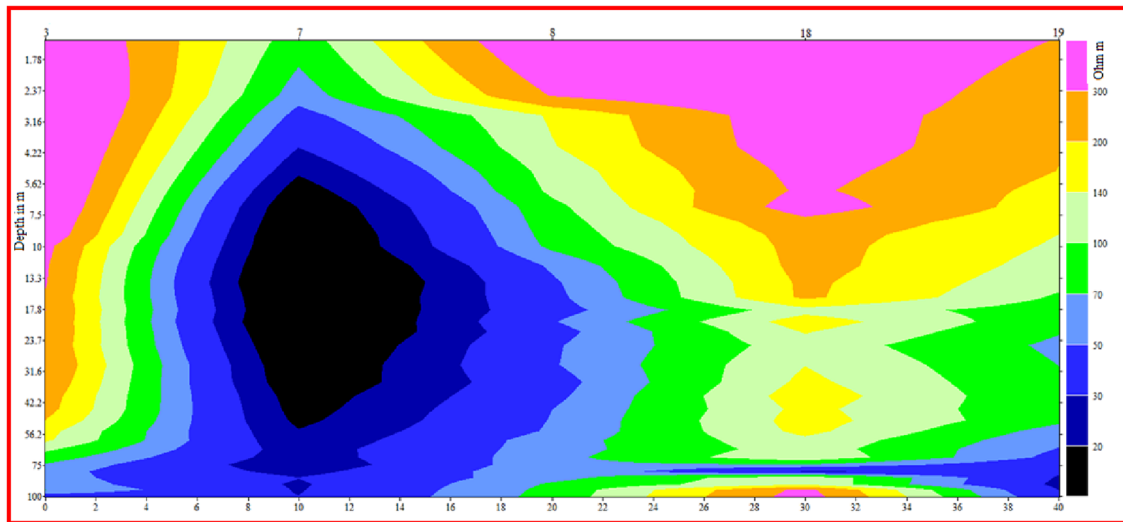


Fig. 10 NE–SW pseudo sections of south west Neyveli Basin

groundwater zone, to delineate the fresh groundwater zones and to examine the saline water intrusion.

Total longitudinal conductance (S) of the southwest Neyveli Basin

Whenever the underlying units show unit conduction, it is possible to measure longitudinal conductance (S) for beds. Groundwater study is carried out over an extended period (Orellena & Mooney, 1966). The letter 'S' variation from VES to VES was used to qualitatively indicate a change in the overall thickness of low-density polyethylene (Shailaja, Kadam, et al., 2019; Suneetha & Gupta, 2018). S values more than one imply competent or consolidated rock, whereas values less than one indicate compact rock at shallower depths. High ' S ' values indicate that the aquifers transmissive are low (Shailaja, Gupta, et al., 2019). The longitudinal values varied from 0.144 to 8.636 (Table 3). The variation of the S value indicates a change in the layers with low resistivity. The following VES sites have a saline water aquifer value > 2 moh (VES nos. 2, 3, 4, 6, 12, 14, 15, 16, and 23). The water aquifer shows that the VES 8, 10, 19, 20, 22, and 24 are modest to freshwater, and they fall into groups of 1.0–2.0 mho, respectively. In the VES 1, 5, 9, 11, 17, 18, 21, 25, and 26, the area covering freshwater is more diminutive than < 1 mho (Fig. 11). As determined by the analysis, the depth of these sounding numbers does not reach the salty aquifer system and is thus excluded from the S value range for the saline groundwater zone. Because of the presence of fresh river sediments the water is unsaturated in shallow depths at the Manimukthanadhi with the Vellar River in the south and east. Because of the presence of laterites in the east Vadalur Sabai, there may be a wide

range of longitudinal conduct in the south and eastern part of the river.

Total transverse unit resistance (T) of southwest Neyveli Basin

The transverse resistance of the total thickness of the saturated aquifer is the vital parameter for an eventual correlation of it with the hydraulic transmissivity. Increasing T values are accompanied by an increase in the thickness of the high resistivity materials. This property ' T ' has been used to indicate the varying thickness of the high resistivity materials and variations in their transverse resistance (Gai-kwad, 2012; Naidu et al., 2021; Shailaja, Gupta, et al., 2019; Suneetha & Gupta, 2018). Increasing ' T ' values are accompanied by an increase in the thickness of the resistivity materials. It has been noticed that increasing T and S has coincided with the high transmissivity of aquifers. The aquifer media's transverse resistance (T) in this area has high ranges from 15.49 to 9289.58 Ωm^2 (Table 3 and Fig. 12). The values are higher along the eastern part of the location in Vadalur Sabai due to laterites in the study area. The range of 1000–4000 Ωm^2 is also considered to identify aquifer zones. The aquifer zones are noted in the north and south, southeast of the study area represents the Tertiary aquifer of the study area. In Nandukuzhi (VES 9) and Vadalur Sabai (VES 23), T values (< 3000) are observed, representing locations of good quality water (Gupta et al., 2014; Patil et al., 2020; Shailaja, Gupta, et al., 2019; Udosen, 2021). Transverse resistance values are often connected with zones of high transmissivity and, consequently, highly permeable zones to fluid flow. The potential aquifer zones in the examined area expand as

Table 3 Aquifer geoelectric properties of the study area

VES no.	Locations	Unit longitudinal conductance (S) in mhos	Aquifer transverse resistance (T) in Ωm^2	Aquifer anisotropy (λ)
1	AgaraAlambadi	0.304	2943.400	9.585
2	Dharmanallur	8.636	15.490	0.877
3	Ko—Adanur	2.430	370.503	1.528
4	Boothamur	2.103	604.040	1.186
5	Pudukuraipettai	0.144	214.001	1.208
6	Eruppukurichchi	2.502	689.880	1.082
7	Kombadikuppam	1.960	212.093	1.660
8	Dhidirkuppam	1.226	1192.430	16.477
9	Nandukuzhi	0.485	4235.150	4.519
10	Kovilankuppam	1.588	2241.282	1.254
11	Vedakovil	0.240	1597.536	1.426
12	Kotteri	3.252	1180.814	2.355
13	Kandiyankuppam	1.106	388.872	1.435
14	Chitherikuppam	2.106	133.080	1.223
15	Mattur	3.871	48.718	1.444
16	Aaladi	3.602	157.039	1.258
17	Kattugudalur	0.977	668.245	1.101
18	Sorattur	0.308	2853.184	6.994
19	Marungur	1.407	282.365	2.578
20	Vadakkumelur	1.088	882.695	1.278
21	Vanadirayapuram	0.254	361.710	1.051
22	Thenkuttu	1.771	344.704	1.138
23	VadalurSabai	7.949	9289.588	1.030
24	Karunkuzhi	1.635	317.030	2.311
25	Seplanattam	0.398	831.718	0.838
26	Guruvesipuram	0.862	640.626	2.133
27	Kammapuram	7.685	1370.497	1.866

transverse resistance increases, most likely due to hydraulic conductivities and electrical anisotropy changes.

Aquifer anisotropy (λ) of southwest Neyveli Basin

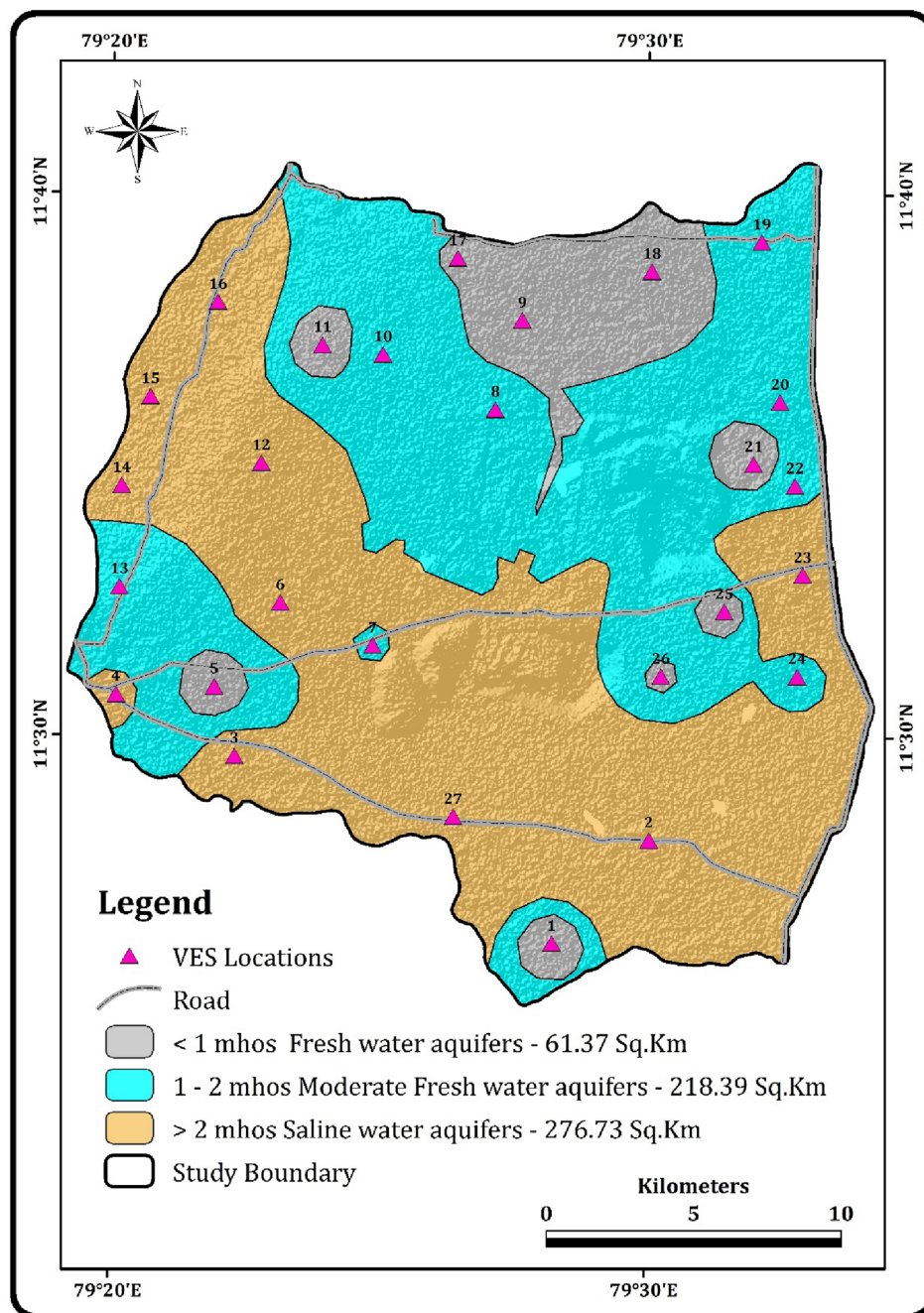
This coefficient is usually greater than 1.00 but does not often exceed 2.00. The ' λ ' can be used as a measure to find out the extent of the anisotropic prevailing in the area of interest. It usually is in the range from 1.02 to 1.10 for Alluvium, 1.05 to 1.15 for Sandstone and Shale, and 1.4 to 2.25 for Slates (Table 4). As the hardness and compaction of rocks increases, the coefficient of anisotropy also increases (Kelter et al., 1966). The aquifer anisotropy (λ) ranges from 0.838 to 16.477, and its spatial distribution is shown (Fig. 13). The value of anisotropy ranging from < 1 (λ) is represented in Dharmanallur and Seplanatham in the south and eastern part of the study area. It indicates the presence of argillaceous materials. The zone with the value of 1 (λ) to 4 (λ) anisotropy exists in most parts of the study area for the possibility of coarse to medium sand. The area with high

anisotropy occurs at the central part of Dhidirkuppam due to the possible occurrence of laterites. Water consumption and management should be enhanced to promote water supply dependability while reducing pollution impacts. As a result, the environment and water supply will be more resilient to the consequences of climate change. These activities will aid coastal protection since agriculture is a major economic engine. Aquifers may be degraded by unregulated agricultural water usage and excessive pumping of coastal aquifers, affecting the health of the residents.

Conclusion

A study of electrical resistivity was conducted at many locations in the Cuddalore district southwest Neyveli Basin to examine the potential of groundwater penetration. The present research explains in greater depth the link between the hydrogeological and geophysical characteristics of groundwater and the findings of a study in the

Fig. 11 Spatial distribution map of total longitudinal conductance (S)



study area. For 27 sites, the VES data has been analyzed using the curve matching method used in the IPI2Win software. From the result, 22% of VES locations dominated by H ($\rho_1 > \rho_2 < \rho_3$) type (VES 2, 5, 6, 11, 21, 22), indicating potential water sites and QH type (VES 3, 7, 10, 20, 23, 24) indicating complex lithology overlain by softer strata, which can be an excellent local for the groundwater potential zone. 19% of HK type (VES 8, 9, 15, 16, 19) indicating $\rho_1 > \rho_2 < \rho_3 > \rho_4$. A-type curves ($\rho_1 < \rho_2 < \rho_3$; VES 1, 4, 17, and 18) fell in 15% of the area, signifying complex rock terrain poor for groundwater storage. Based

on this interpretation, this study shows the effectiveness of the electrical resistivity method in identifying prospective groundwater zones. The VES survey may characterize subsurface layers and design groundwater development plans. These characteristics will assist in determining the salty and freshwater aquifer zones. Thus, these factors reduce uncertainty by interpreting and restricting the borders between various groundwater zones. As a result of saltwater intrusion, the freshwater zone in Archean and Tertiary strata is saline. Using DZ characteristics, the study proposes a viable way to delineate the freshwater

Fig. 12 Spatial distribution map of total transverse unit resistance (*T*)

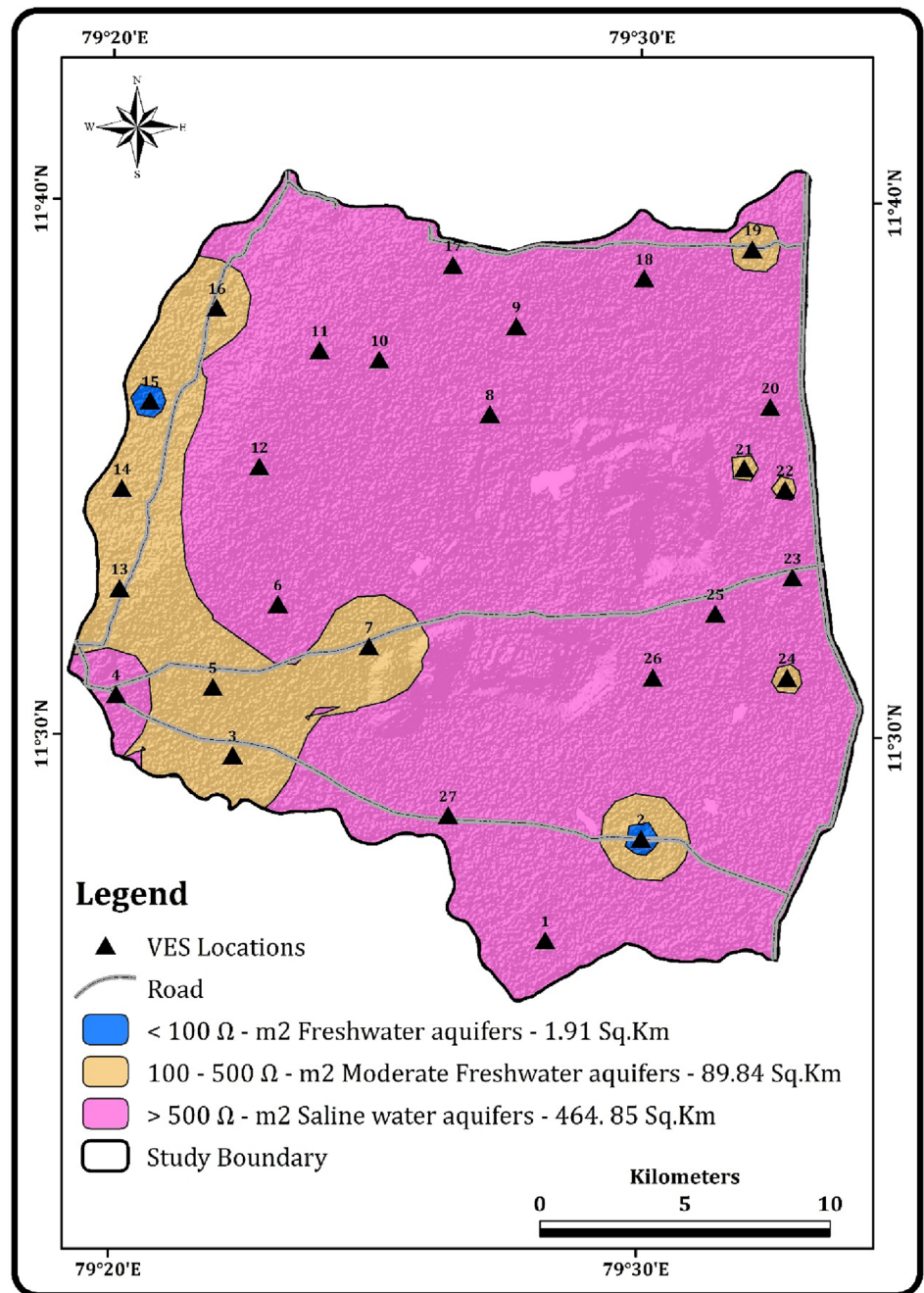
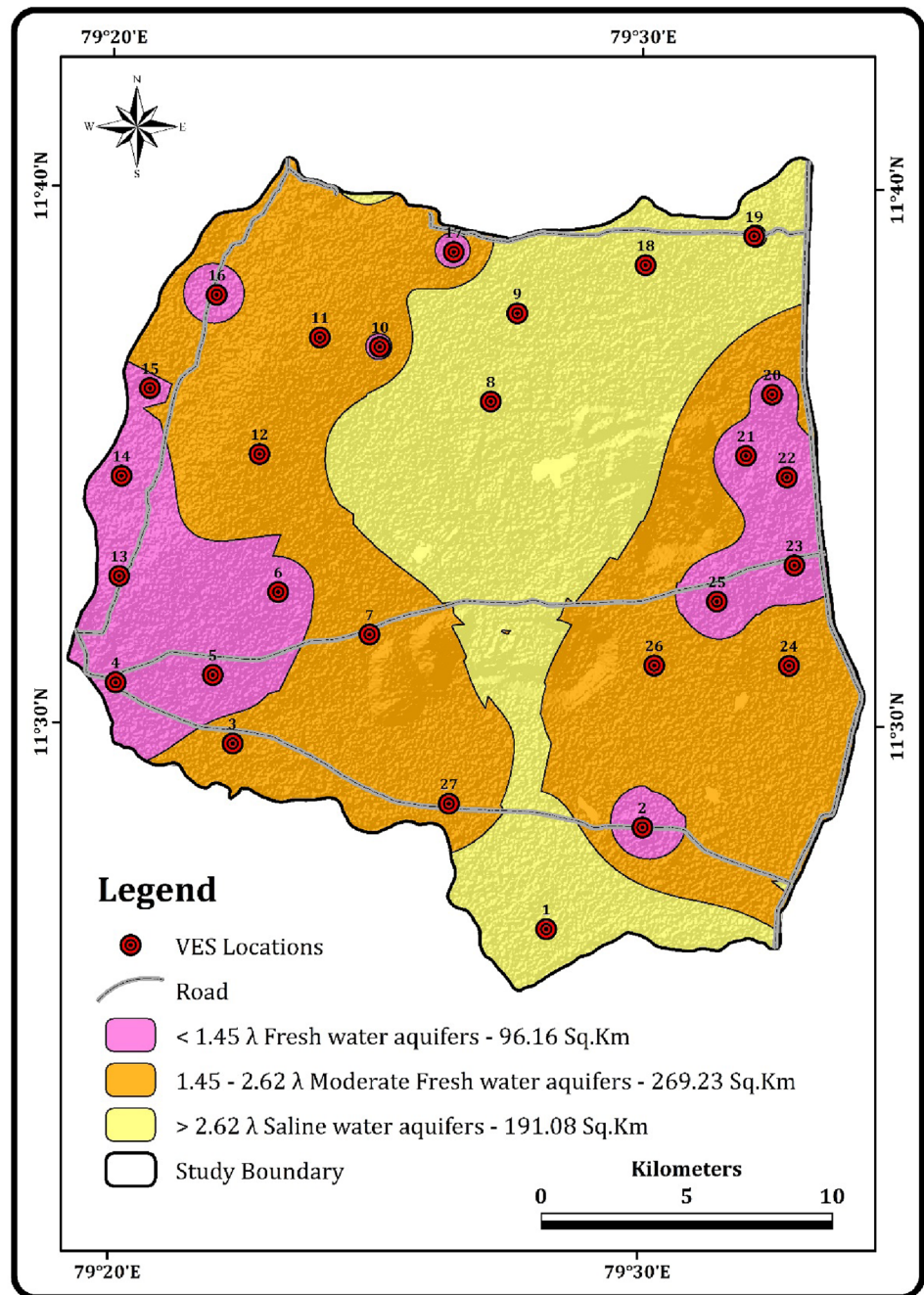


Table 4 Anisotropy coefficient value for different aquifer lithology (Singh et al., 2021)

Sl. No.	Aquifer lithology	Anisotropy value (λ)
1.	Alluvium	1.02–1.10
2.	Sandstone and shale	1.05–1.15
3.	Slates	1.40–2.25
4.	Graphite	2.0–2.8
5.	Intrusive bodies like, dyke, sill batholiths	> 2.0
6.	Interbedded anhydrite and shale	4.0–7.5

and saltwater aquifers. These indicators also give a trustworthy explanation, especially when the resistivity data analysis is hampered by the intermixing of resistivity of the area salty and fresh fluids, clayey and sandy layers in any coastal aquifer system. The delineation of the aquifer and the hydro-geologic characterization of groundwater resources in a Neyveli Basin effectively manage and conserves groundwater resources.

Fig. 13 Spatial distribution map of aquifer anisotropy (λ)



Acknowledgements The authors wish to thank all who assisted in conducting this work.

References

- Anbazhagan, S., Indhirajith, R., Uma Maheshwaran, S., Jothibas, A., Venkatesan, A., & Ramesh, V. (2015). Electrical resistivity survey and shallow subsurface geological study in hard rock terrain, Southern India. *Journal of the Geological Society of India*. <https://doi.org/10.1007/s12594-015-0219-2>
- Arunbose, S., Srinivas, Y., & Rajkumar, S. (2021). Efficacy of hydrological investigation in Karumeniyar river basin, Southern Tamil Nadu, India using vertical electrical sounding technique: A case study. *Methods X*. <https://doi.org/10.1016/j.mex.2021.101215>
- Ayolabi, E. A., Folorunso, A. F., & Oloruntola, M. O. (2010). Constraining causes of structural failure using electrical resistivity tomography (ERT): A case study of Lagos, southwestern Nigeria. *Mineral Wealth*, 156, 7–18.
- Bello, R., Balogun, A. O., & Nwosu, U. M. (2019). Evaluation of Dar zarrouk parameters of parts of Federal University of Petroleum Resources, Effurun, Nigeria. *Journal of Applied Sciences and Environmental Management*. <https://doi.org/10.4314/jasem.v23i9.16>

- Chatterjee R, Purohit RR (2009) Estimation of replenishable groundwater resources of India and their status of utilization. *Current Science*, 96 (12), 1581–1591.
- Chopra, A., & Ramachandran, P. (2021). Understanding water institutions and their impact on the performance of the water sector in India. *Water Policy*. <https://doi.org/10.2166/wp.2021.207>
- Devaraj, N., Chidambaram, S., Panda, B., et al. (2018). Geo-electrical approach to determine the lithological contact and groundwater quality along the KT boundary of Tamil Nadu, India. *Modeling Earth Systems and Environment*. <https://doi.org/10.1007/s40808-018-0424-2>
- Gaikwad, S. K. (2012). *Geochemistry of fluoride bearing ground waters from the Karli River Basin, Southern part of Sindhudurg District, Maharashtra*. Unpublished PhD thesis, Department of Geology, University of Pune.
- Gaikwad, S., Pawar, N. J., Bedse, P., Wagh, V., & Kadam, A. (2021). Delineation of groundwater potential zones using vertical electrical sounding (VES) in a complex bedrock geological setting of the West Coast of India. *Modeling Earth Systems and Environment*. <https://doi.org/10.1007/s40808-021-01223-3>
- Golekar, R. B., Patil, S. N., Kachate, N. R., & Diwate, P. (2021). Geospatial distribution of dar zarrouk parameters resulting from vertical electrical sounding in Dharangaon and Erandol Block of Jalgaon District, India. In Varun Narayan Mishra (Eds.), *Geoinformation technology in earth resources monitoring and management*. Nova Science Publishers Inc
- Gopinath, S., & Srinivasamoorthy, K. (2014). *Geophysical VES approach for seawater intrusion assessment in Nagapattinam and Karaikal coastal aquifers, India. Coastal resources and management strategies through spatial technology* (pp. 50-56.22). Villapuram: Iyal Publications.
- Gopinath, S., Srinivasamoorthy, K., Saravanan, K., & Prakash, R. (2018). Discriminating groundwater salinization processes in coastal aquifers of southeastern India: Geophysical, hydro-geochemical and numerical modeling approach. *Environment, Development and Sustainability*. <https://doi.org/10.1007/s1068-018-0143-x23>
- Gopinath, S., Srinivasamoorthy, K., Saravanan, K., Suma, C. S., Prakash, R., Senthinathan, D., & Sarma, V. S. (2017). Vertical electrical sounding for mapping saline water intrusion in coastal aquifers of Nagapattinam and Karaikal, South India. *Sustainable Water Resources Management*. <https://doi.org/10.1007/s40899-017-178-4>
- Gupta, G., Maiti, S., & Erram, V. C. (2014). Analysis of electrical resistivity data in resolving the saline and freshwater aquifers in west coast Maharashtra. *Journal of the Geological Society of India*, 84(5), 555–568.
- Hazarika, N., & Nitivattananon, V. (2016). Strategic assessment of groundwater resource exploitation using DPSIR framework in Guwahati city, India. *Habitat International*. <https://doi.org/10.1016/j.habitatint.2015.10.003>
- Kalaivanan, K., Gurugnanam, B., Pourghasemi, H. R., Suresh, M., & Kumaravel, S. (2018). Spatial assessment of groundwater quality using water quality index and hydrochemical indices in the Kodavanan sub-basin, Tamil Nadu, India. *Sustainable Water Resources Management*, 4, 627–641. <https://doi.org/10.1007/s40899-017-0148-x>
- Kalaivanan, K., Gurugnanam, B., & Suresh, M. (2019). Geoelectrical resistivity investigation for hydrogeology conditions and groundwater potential zone mapping of Kodavanan sub-basin, southern India. *Sustainable Water Resources Management*. <https://doi.org/10.1007/s40899-019-00305-6>
- Kavidha, R., & Elangovan, K. (2013). Delineation of groundwater prospective zones by electrical resistivity method in Erode District, Tamil Nadu, India. *Journal of Environment*
- Keller, G. V., & Frischknecht, F. C. (1966). *Electrical methods in geophysical prospecting*. New York: Pergamon.
- Kolandhavel, P., & Ramamoorthy, S. (2019). Investigation of groundwater potential zones in NandiAru Sub Basin, Tamil Nadu, India—An integrated geophysical and geoinformatics approach. *Arabian Journal of Geosciences*. <https://doi.org/10.1007/s12517-019-4247-x>
- Kumar, R., & Yadav, G. S. (2015). Geohydrological investigation using Schlumberger sounding in part of hard rock and alluvial area of Ahraura region, Mirzapur district, Uttar Pradesh, India. *Arabian Journal of Geosciences*. <https://doi.org/10.1007/s12517-014-1447-2>
- Latha, J., Saravanan, S., & Palanichamy, K. (2010). A semi-distributed water balance model for Amaravathi River Basin using remote sensing and GIS. *International Journal of Geomatics and Geosciences*, 1, 252.
- Lawal, A., Tijani, M. N., & D'Alessio, M. (2020). Geoelectrical characterisation of aquifers in Bauchi-Alkaleri-Kirfi geological transition zones, Northeast Nigeria. *Environmental Earth Sciences*. <https://doi.org/10.1007/s12665-020-08978-5>
- Maity, P. K., Das, S., & Das, R. (2017). Methodology for groundwater extraction in the coastal aquifers of Purba Midnapur District of West Bengal in India under the constraint of saline water intrusion. *Asian Journal of Water, Environment and Pollution*. <https://doi.org/10.3233/AJW-170011>
- Mathiazhagan, M., Selvakumar, T., & Madhavi, G. (2015). Surface geo-electrical sounding for the determination of aquifer characteristics in part of the Palar Sub-Basin, Tamil Nadu, India. *Journal of Chemical and Pharmaceutical Sciences*, 974, 2115.
- Mondal, N. C. (2021). Geoelectrical signatures for detecting water-bearing zones in a micro-watershed of granitic terrain from Southern India. *Journal of Applied Geophysics*. <https://doi.org/10.1016/j.jappgeo.2021.104361>
- Nagaraju, D., Mahadevaswamy, G., Siddalingamurthy, S., Nagesh, P. C., Rao, K., & Pankaja, G. V. (2011). Groundwater development studies using remote sensing and GIS techniques in drought prone area of Chamarajanagar district, Karnataka, India. *Nature, Environment and Pollution Technology*, 10, 661–664.
- Nageswara Rao, P. V., Appa Rao, S., & Subba Rao, N. (2018). Delineation of groundwater prospective zones from a delta region of India, using geoelectrical and water quality approach. *Environmental Earth Sciences*. <https://doi.org/10.1007/s12665-018-7786-7>
- Naidu, S., Gupta, G., Shailaja, G., & Tahama, K. (2021). Spatial behavior of the Dar-Zarrouk parameters for exploration and differentiation of water bodies aquifers in parts of Konkan coast of Maharashtra, India. *Journal of Coastal Conservation*, 25(1), 1–9. <https://doi.org/10.1007/s11852-021-00807-6>
- Ndatuwong, L. G., & Yadav, G. S. (2015). Application of geo-electrical data to evaluate groundwater potential zone and assessment of overburden protective capacity in part of Sonebhadra district, Uttar Pradesh. *Environmental Earth Sciences*. <https://doi.org/10.1007/s12665-014-3649-z>
- Omosuyi, G. O., Oshodi, D. R., Sanusi, S. O., & Adeyem, I. A. (2021). Groundwater potential evaluation using geoelectrical and analytical hierarchy process modeling techniques in Akure-Owode, southwestern Nigeria. *Modeling Earth Systems and Environment*, 7, 145–158. <https://doi.org/10.1007/s40808-020-00915-6>
- Orellena, E., & Mooney, H. M. (1966). *Master tables and curves of vertical electrical sounding over layered structures* (pp. 150–166). Madrid: Interciencia.
- Panda, B., Chidambaram, S., & Ganesh, N. (2017). An attempt to understand the subsurface variation along the mountain front and riparian region through geophysics technique in South India. *Modeling Earth Systems and Environment*. <https://doi.org/10.1007/s40808-017-0334-8>

- Patil, S. N., Kachate, N. R., & Ingle, S. T. (2018). Estimation of Da-Zarrouk parameters for groundwater exploration in parts of Chopda Taluka, Jalgaon district, Maharashtra (India). *Journal of Indian Geophysical Union (july 2018)*, 22, 425–435.
- Patil, V. B., Lokesh, K. N., Krishnamurthy, M. P., & Nadagoudar, H. V. (2020). Delineation of groundwater potential zones using integrated approach in semi-arid hard rock terrain, Kanavi Halla Sub-Basin, Belagavi District, Karnataka. *Journal of the Geological Society of India*, 96(4), 410–419.
- Prabhu, K., & Sivakumar, R. (2018). Geoelectrical resistivity survey for groundwater potential—A case study of Nandi river basin, Tamil Nadu, India. *Applied Ecology and Environmental Research*. https://doi.org/10.15666/aeer/1602_19611972
- Ravi, R., Aravindan, S., Ramachandran, C., Balabantaray, S. K., Selvaraj, B., & Santhakumar, K. (2021). Pore resistivity variation by Resistivity imaging technique in sedimentary part of main Gadilam river basin, Cuddalore District, Tamil Nadu, India. *Journal of Applied and Natural Science*. <https://doi.org/10.31018/jans.v13i1.2541>
- Sampat, P. (2000). Groundwater shock: The polluting of the world's major freshwater stores. *World Watch*, Jan–Feb, 10–22.
- Sathiyamoorthy, M., & Ganesan, M. (2018). Delineation of groundwater potential and recharge zone using electrical resistivity method around Veeranam Tank, Tamil Nadu, India. *Journal of the Institution of Engineers (india): Series A*. <https://doi.org/10.1007/s40030-018-0318-3>
- Selvakumar, T., Mathiazhagan, M., & Ganesan, M. (2015). Geoelectrical resistivity survey of the Chennai Sewage Treatment plants for identifying reclaimed water recharge. *Journal of Coastal Sciences*, 2, 19–23.
- Senthilkumar, S., Gowtham, B., & Vinodh, K. (2017). Delineation of subsurface layers using resistivity imaging techniques in coastal blocks of Thiruvallur District, Tamil Nadu, India. *Indian Journal of Geo-Marine Sciences*, 46, 986–994.
- Senthilkumar, S., Vinodh, K., & Johnson Babu, G. (2019). Integrated seawater intrusion study of coastal region of Thiruvallur district, Tamil Nadu, South India. *Applied Water Science*. <https://doi.org/10.1007/s13201-019-1005-x>
- Shailaja, G., Gupta, G., Suneetha, N., & Laxminarayana, M. (2019). Assessment of aquifer zones and its protection via second-order geoelectric indices in parts of drought-prone region of Deccan Volcanic Province, Maharashtra. *India. J Earth Syst Sci*, 128(4), 1–18.
- Shailaja, G., Kadam, A. K., Gupta, G., Umrikar, B. N., & Pawar, N. J. (2019). Integrated geophysical, geospatial and multiple-criteria decision analysis techniques for delineation of groundwater potential zones in a semi-arid hard-rock aquifer in Maharashtra, India. *Hydrogeology Journal*, 27(2), 639–654.
- Singh, S., Gautam, P. K., & Kumar, P. (2021). Delineating the characteristics of saline water intrusion in the coastal aquifers of Tamil Nadu, India by analyzing the Dar-Zarrouk parameters. *Contributions to Geophysics and Geodesy*. <https://doi.org/10.31577/congeo.2021.51.2.3>
- Suneetha N, Gupta G (2018) *Evaluation of groundwater potential and saline water intrusion using secondary geophysical parameters: A case study from western Maharashtra, India*. In: E3S web of conferences, Vol. 54. EDP Sciences, p 33
- Udosen, N. L. (2021). Geo-electrical modeling of leachate contamination at a major waste disposal site in South-Eastern Nigeria. *Modeling Earth Systems and Environment*. <https://doi.org/10.1007/s40808-021-01120-9>
- Utom, A. U., Odoh, B. I., & Okoro, A. U. (2012). Estimation of aquifer transmissivity using Dar Zarrouk parameters derived from surface resistivity measurements: A case history from parts of Enugu Town (Nigeria). *Journal of Water Resource and Protection*. <https://doi.org/10.4236/jwarp.2012.412115>
- Verma, R. K., Bhuin, N. C., & Rao, C. V. (1980). Use of electrical resistivity methods for study of some faults in the Jharia coalfield, India. *Geoexploration*, 18, 201–220.